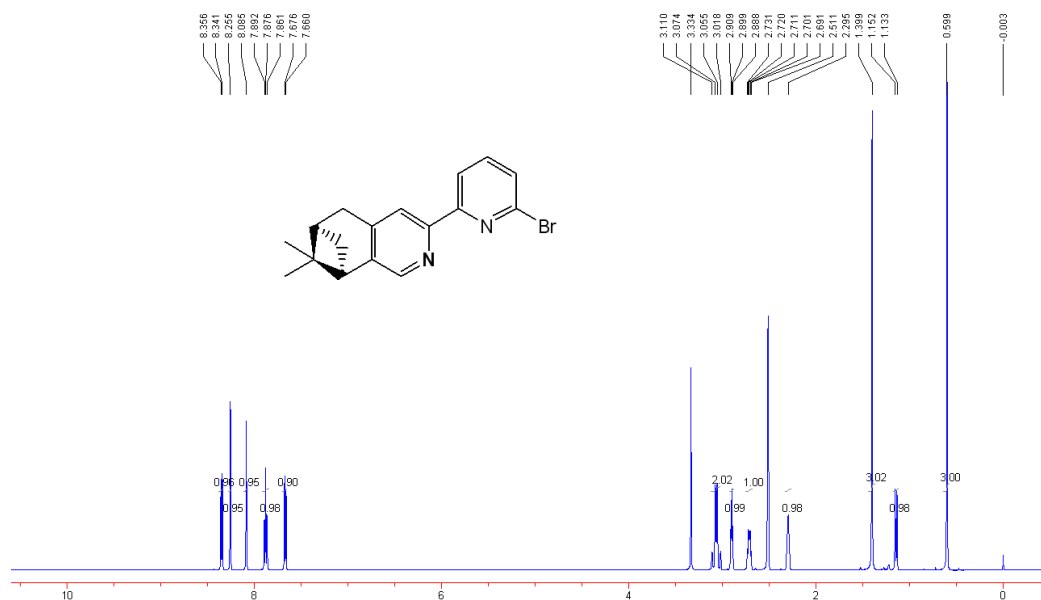


## Supporting Information

### Vapor-induced Chiroptical Switching in Chiral Cyclometalated Platinum(II) Complexes with Pinene Functionalized C<sup>N</sup>N Ligands

Xiao-Peng Zhang, Tao Wu, Jian Liu, Jing-Xuan Zhang, Cheng-Hui Li\*, Xiao-Zeng You\*

<sup>†</sup>State Key laboratory of Coordination Chemistry, School of Chemistry and Chemical Engineering, Nanjing National Laboratory of Microstructures Nanjing University, Nanjing 210093, People's Republic of China. E-mail: chli@nju.edu.cn (C. -H. Li); youxz@nju.edu.cn (X.-Z. You.)



**Fig. S1** <sup>1</sup>H NMR spectrum of (-)-4,5-pinene-6'-bromo-2,2'-bipyridine.

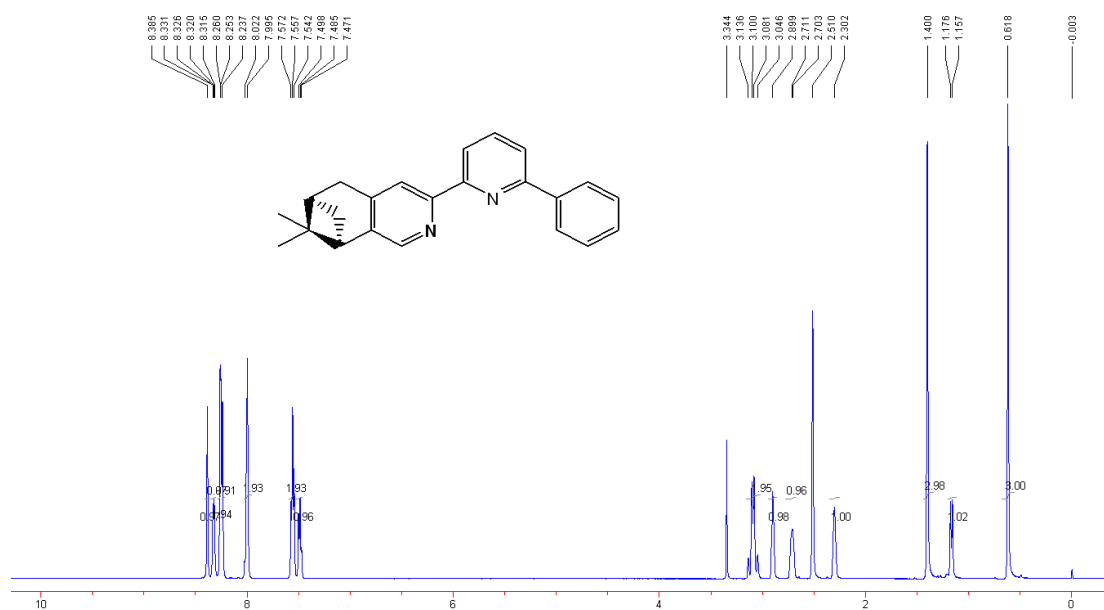


Fig. S2  $^1\text{H}$  NMR spectrum of (-)-4,5-pinene-6'-phenyl-2,2'-bipyridine ( $L_a$ ).

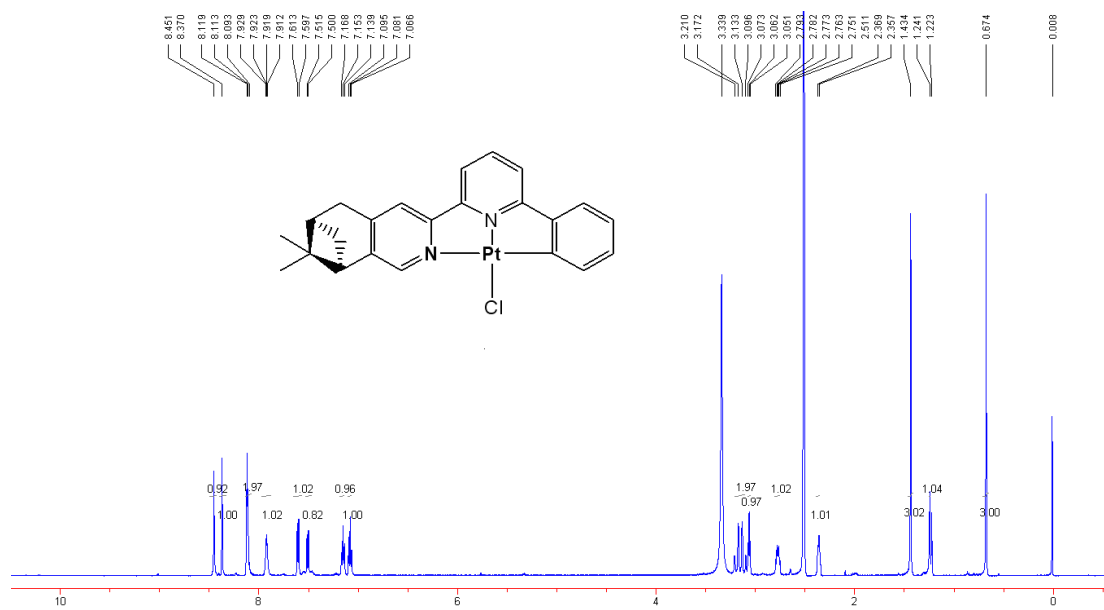


Fig. S3  $^1\text{H}$  NMR spectrum of  $\text{Pt}(L_a)\text{Cl}$ .

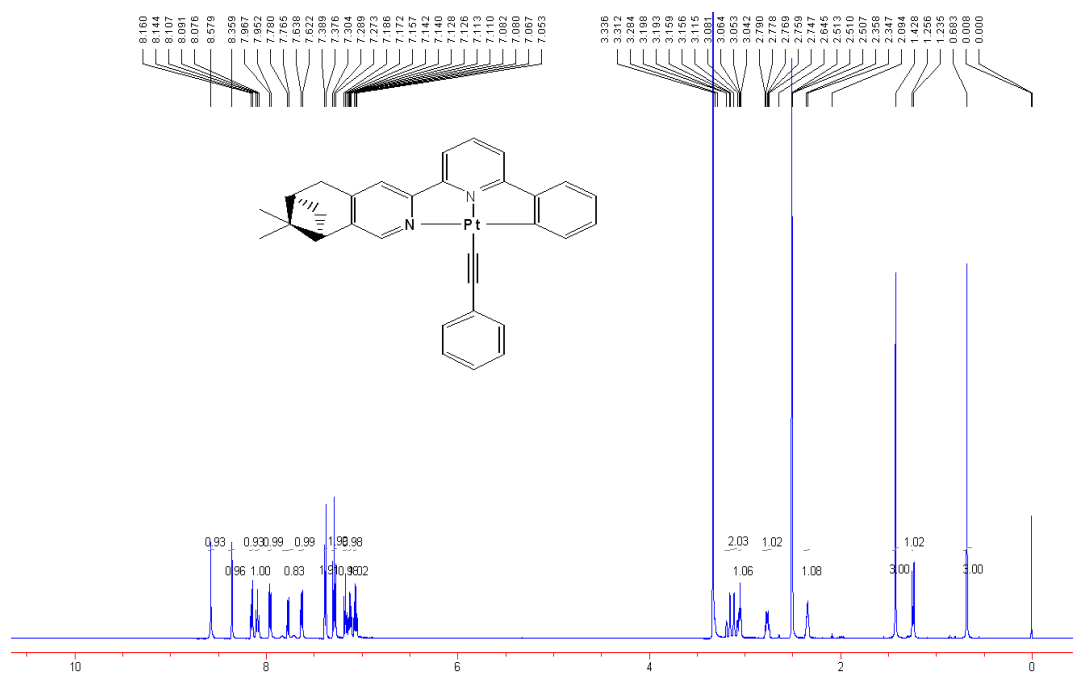


Fig. S4  $^1\text{H}$  NMR spectrum of  $\text{Pt}(\text{L}_a)(\text{C}\equiv\text{C}-\text{Ph})$  (**1a**).

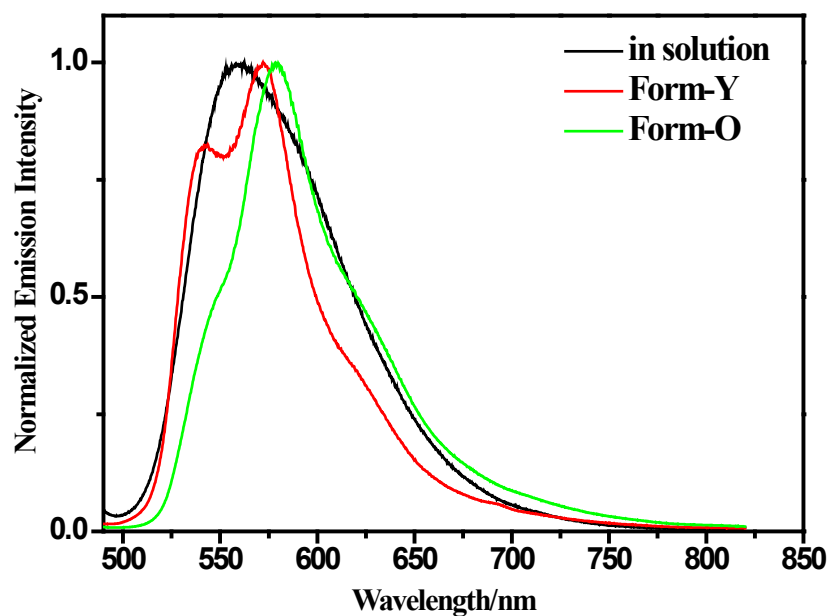
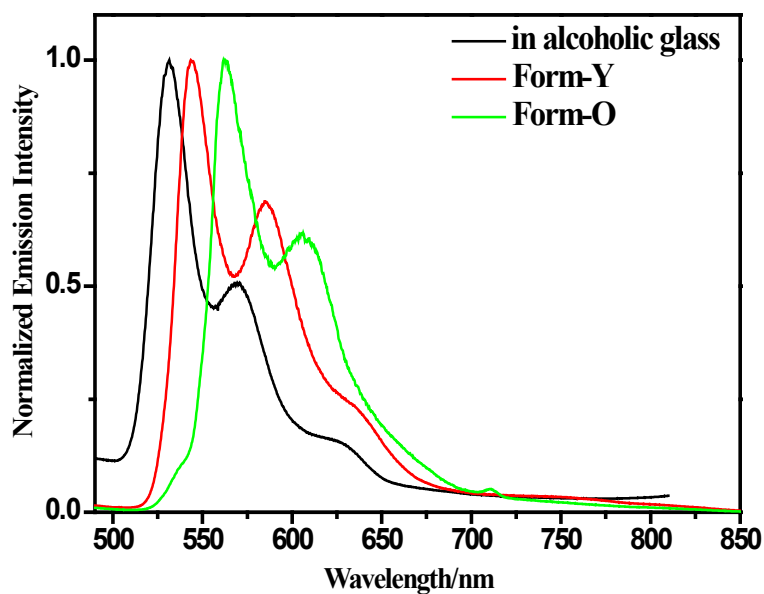
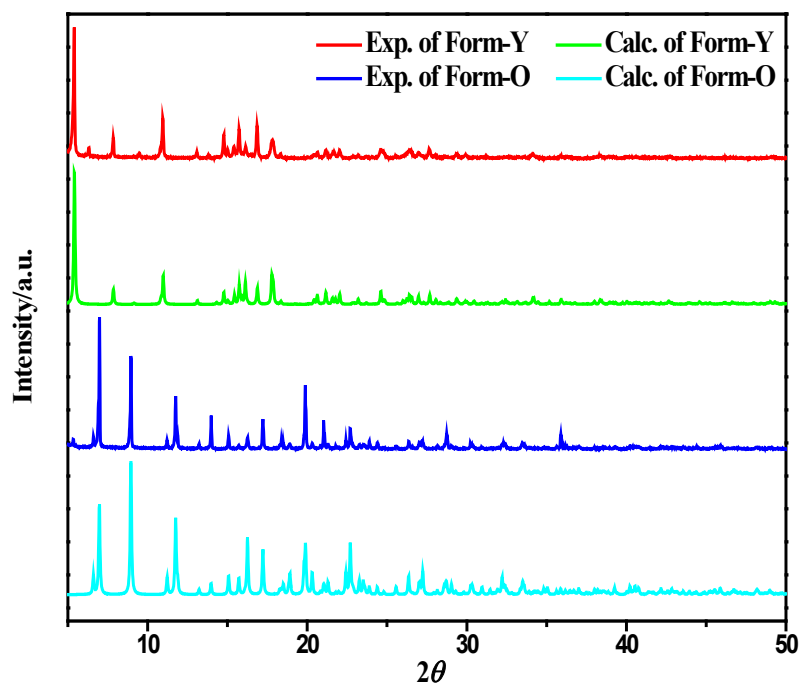


Fig. S5 Emission spectra of **1a** in solution ( $10^{-5} \text{ mol}\cdot\text{L}^{-1}$ ) and different solid-state forms at 298K (in acetonitrile solution at 298K,  $\lambda_{\text{ex}} = 420 \text{ nm}$ ; **Form-Y**: yellow crystallites,  $\lambda_{\text{ex}} = 460 \text{ nm}$ ; **Form-O**: orange crystallites,  $\lambda_{\text{ex}} = 470 \text{ nm}$ ).



**Fig. S6** Emission spectra of **1a** in alcoholic glass ( $10^{-5}$  mol·L $^{-1}$ ) and different solid-state forms at 77K (in MeOH : EtOH (v/v = 1:4) glass,  $\lambda_{\text{ex}} = 420$  nm; **Form-Y**: yellow crystallites,  $\lambda_{\text{ex}} = 460$  nm; **Form-O**: orange crystallites,  $\lambda_{\text{ex}} = 470$  nm).



**Fig. S7** Simulated and experimental XRD patterns of complex **1a** with different forms. (**Form-Y**: yellow crystallites; **Form-O**: orange crystallites)

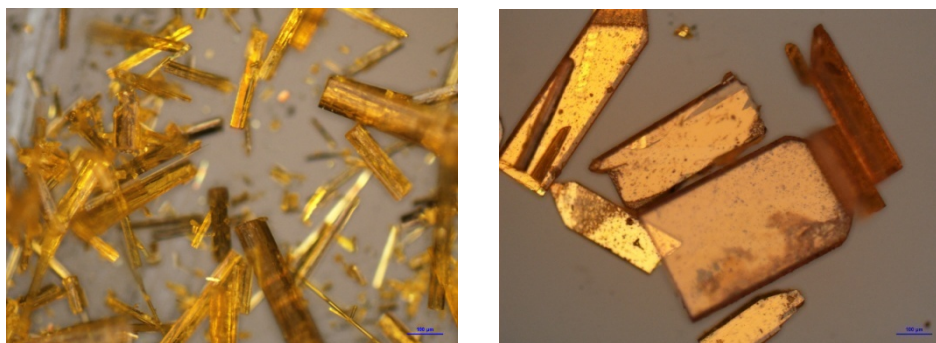


Fig. S8 Crystal pictures of **1a-Form-Y** (left) and **1a-Form-O** (right).

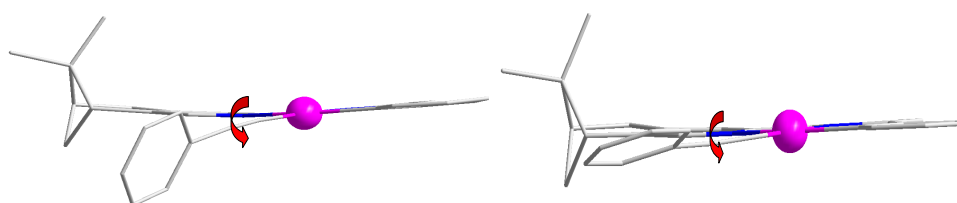


Fig. S9 Absolute configurations of **1a-Form-Y** (left) and **1a-Form-O** (right) based on skew-line system, and both of them are  $\Lambda$ .

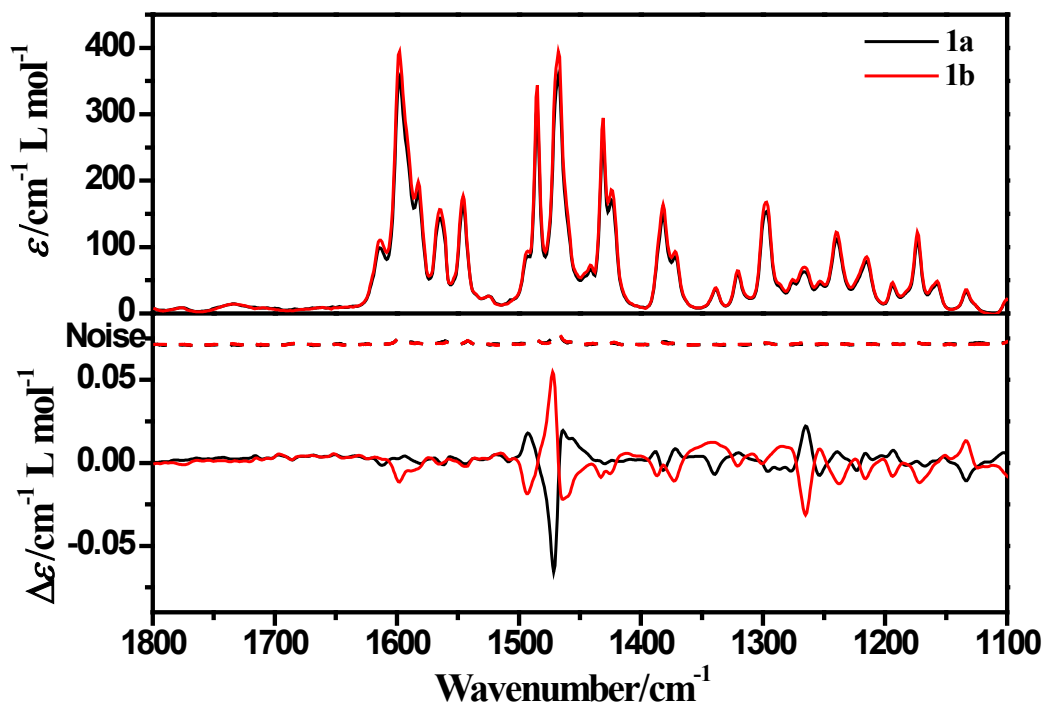


Fig. S10 IR and VCD spectra of complexes **1a** and **1b** in CDCl<sub>3</sub> solution.

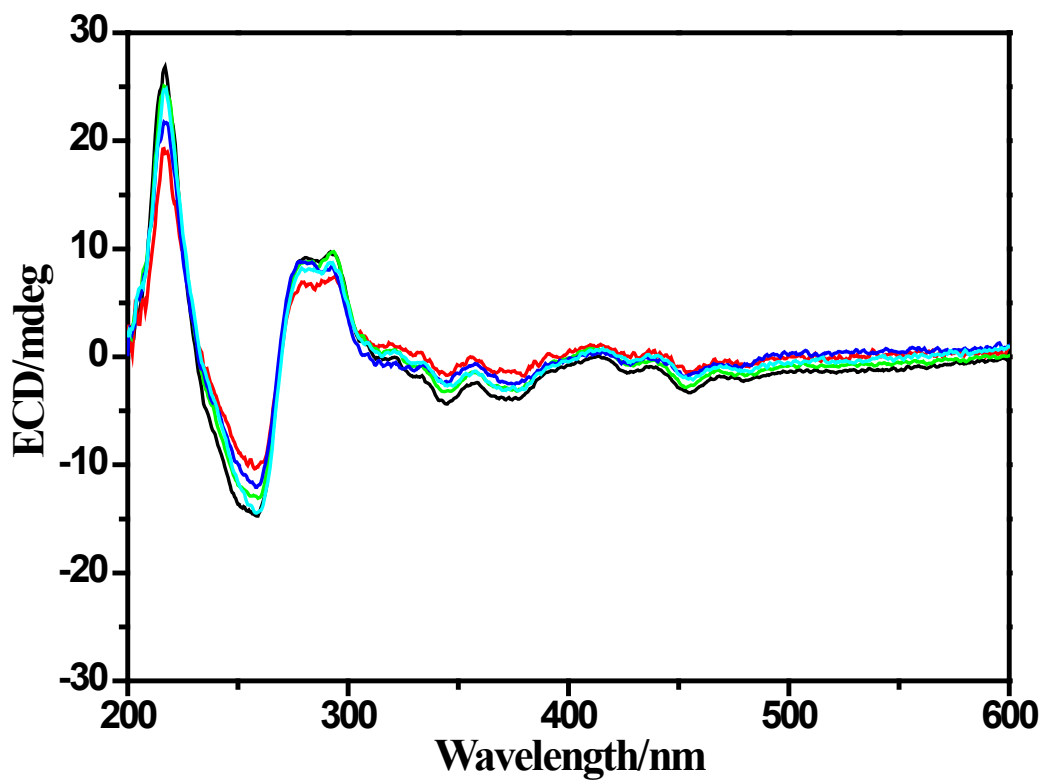


Fig. S11 Five groups solid-state ECD spectra of **Form-Y** of **1a** under the same measuring condition.

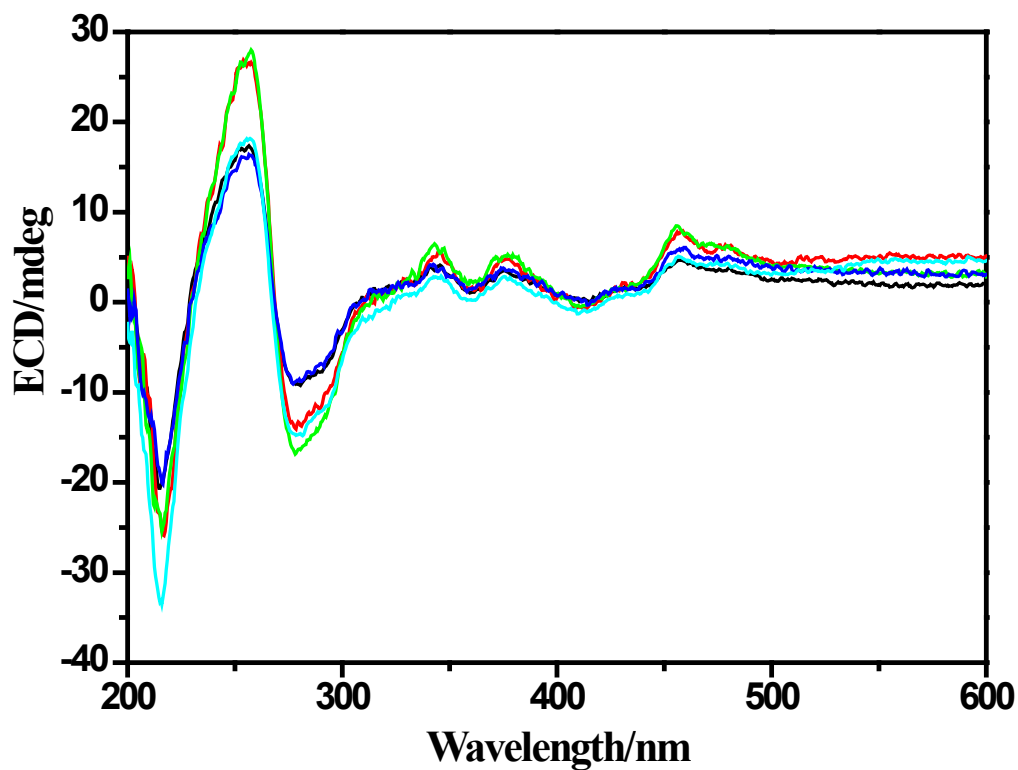


Fig. S12 Five groups solid-state ECD spectra of **Form-Y** of **1b** under the same measuring condition.

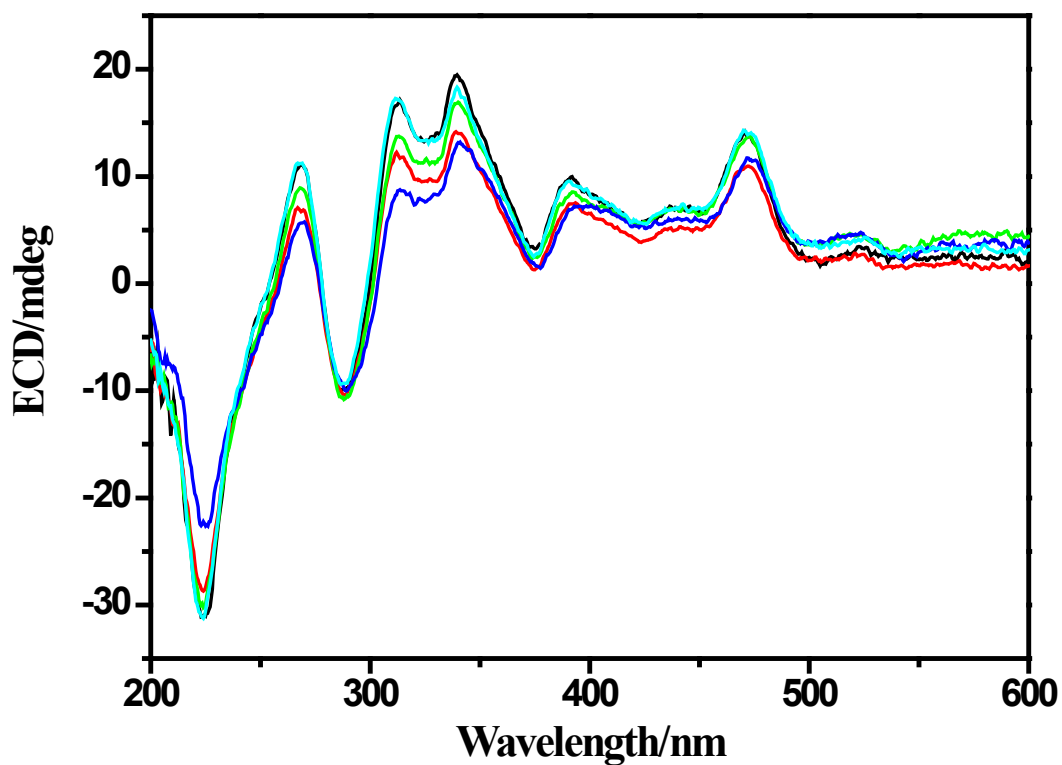


Fig. S13 Five groups solid-state ECD spectra of Form-O of **1a** under the same measuring condition.

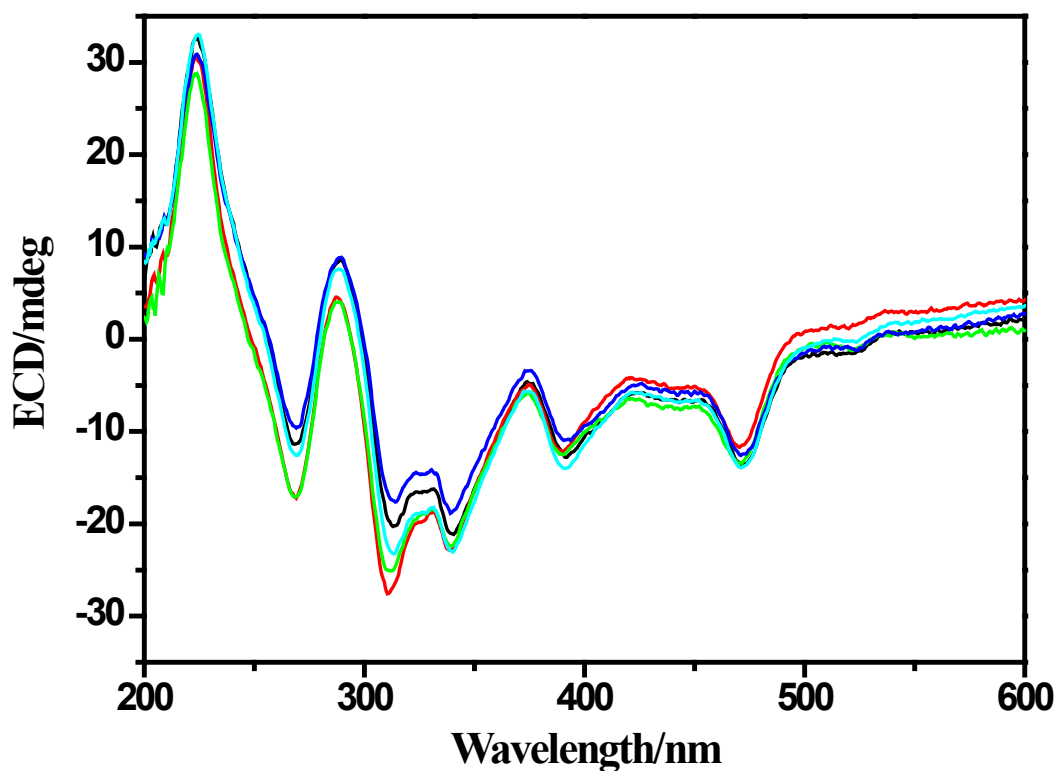
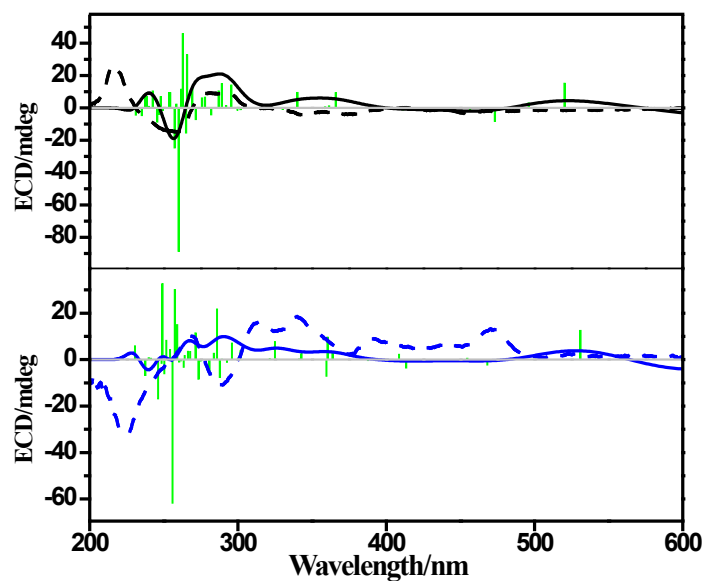
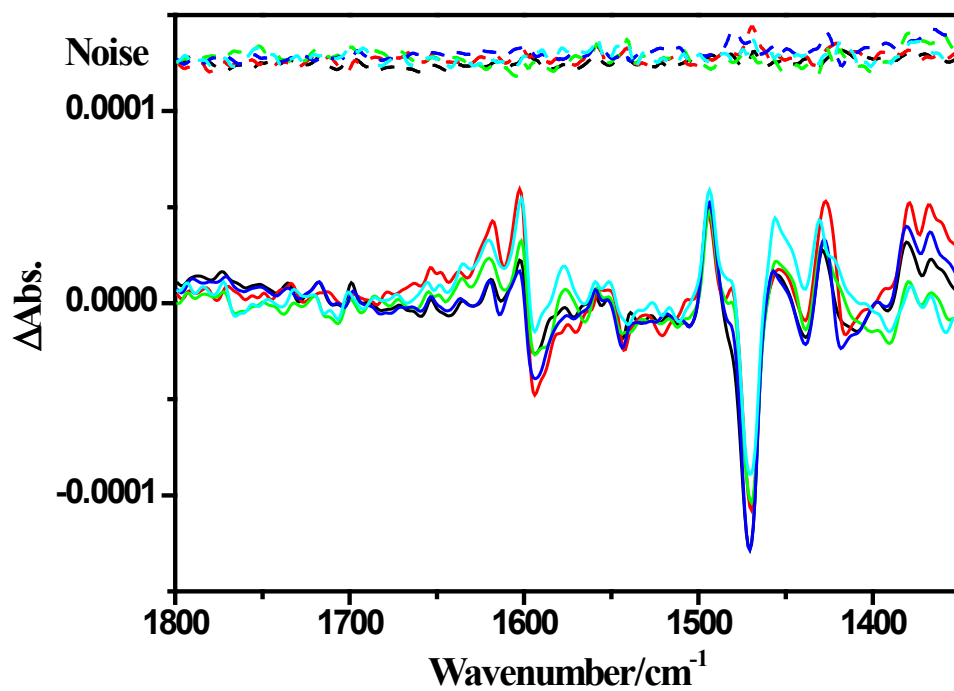


Fig. S14 Five groups solid-state ECD spectra of Form-O of **1b** under the same measuring condition.



**Fig. S15** Computed ECD spectra (solid line) of **Form-Y** (black) and **Form-O** (blue) of complex **1a** compared to observed solid-state ECD spectra (dash line). The green column is the computed rotatory strength.



**Fig. S16** Five groups solid-state VCD spectra of **Form-Y** of **1a** under the same measuring condition (solid line: VCD spectra; dashed line: noise level).



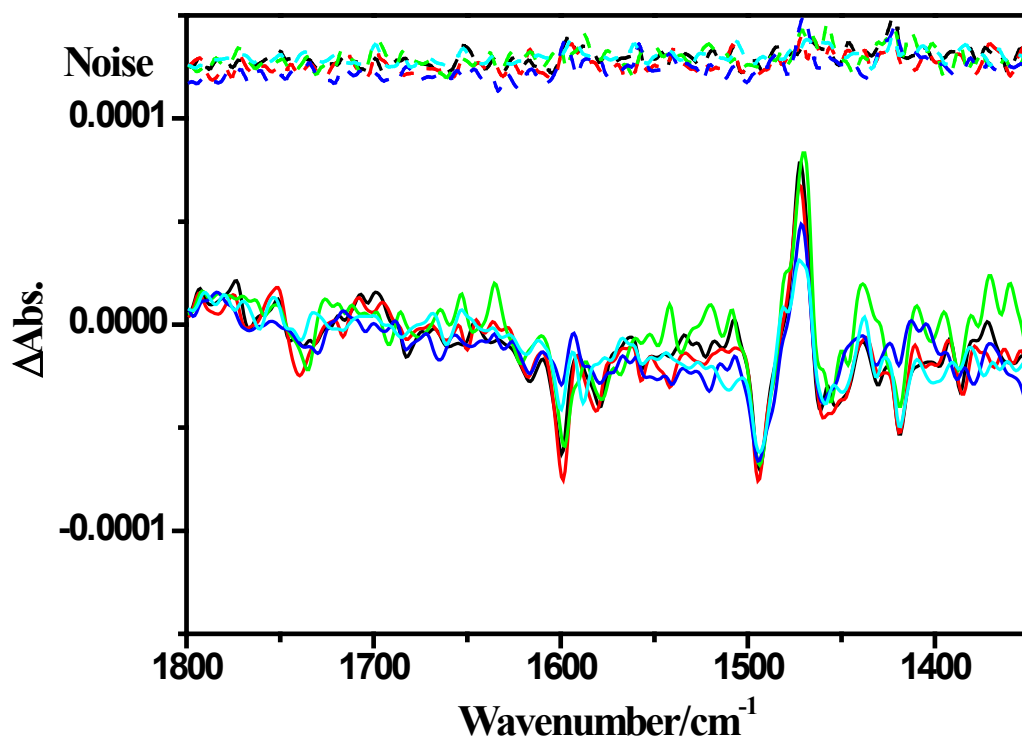


Fig. S17 Five groups solid-state VCD spectra of **Form-Y** of **1b** under the same measuring condition (solid line: VCD spectra; dashed line: noise level).

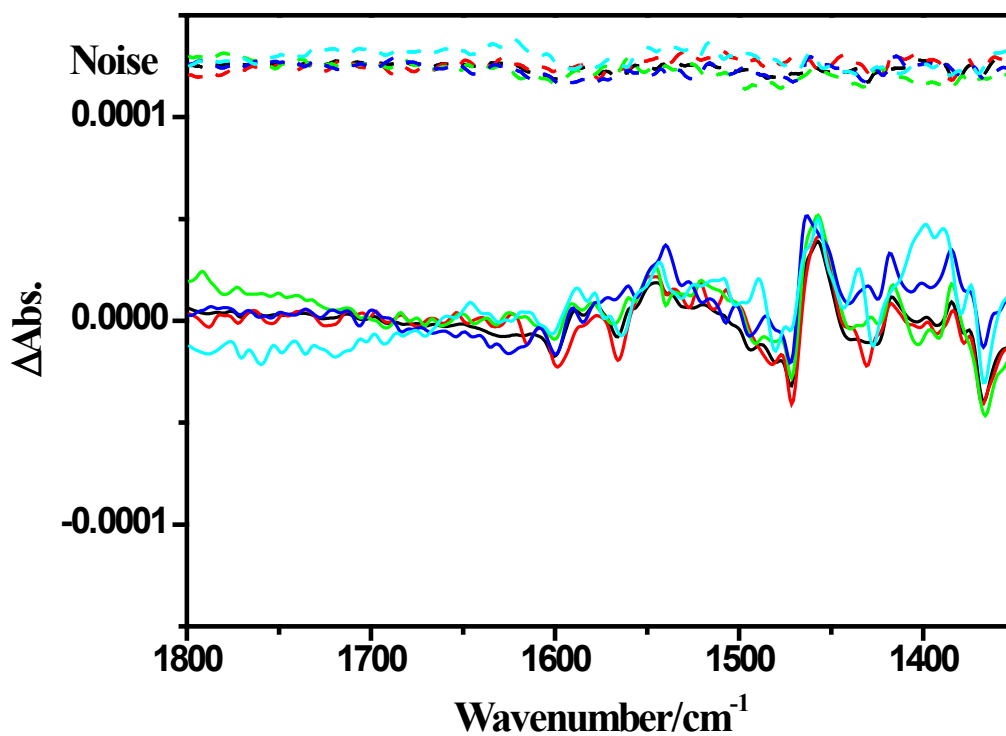
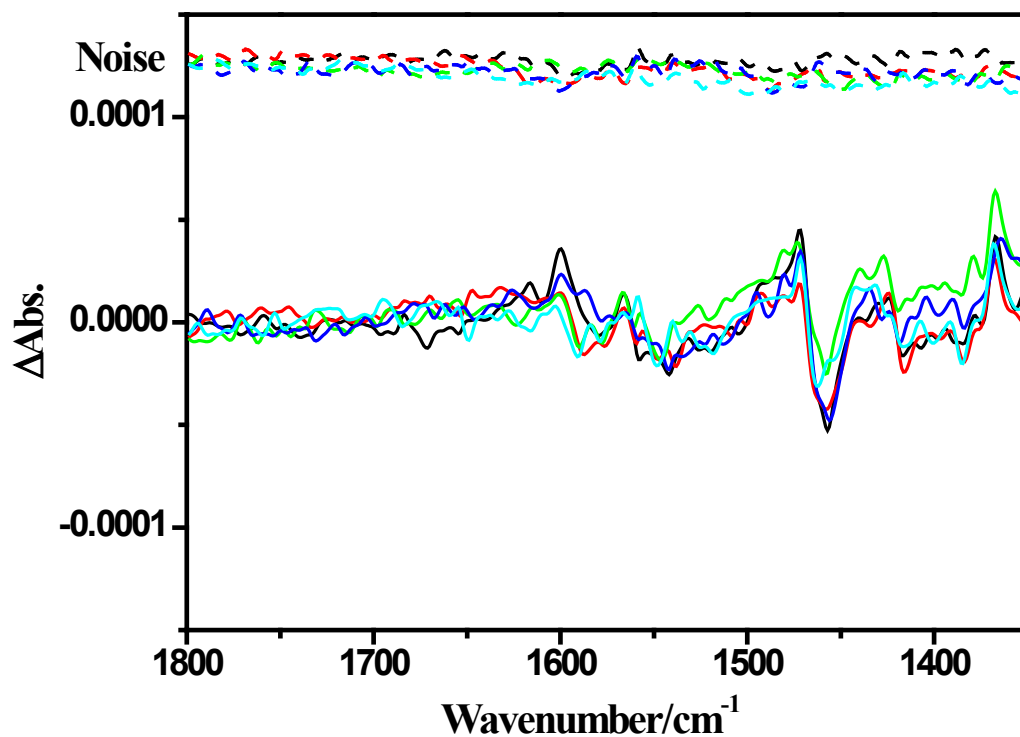
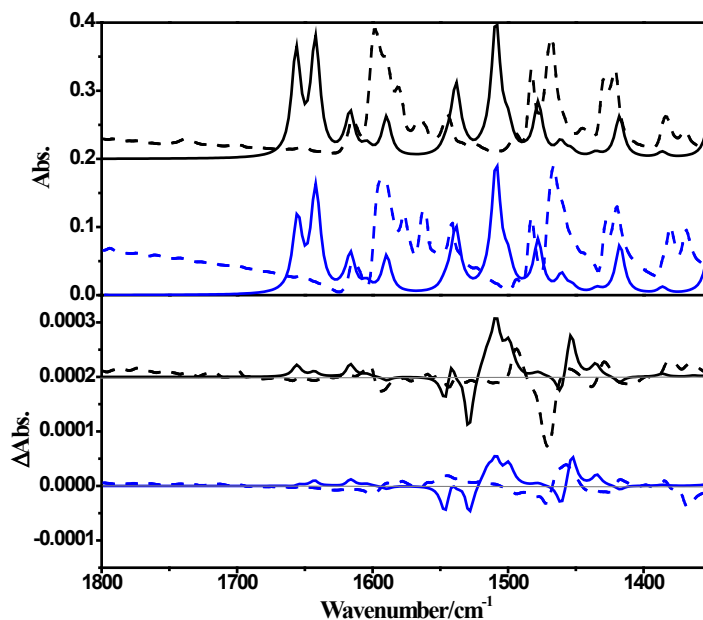


Fig. S18 Five groups solid-state VCD spectra of **Form-O** of **1a** under the same measuring condition (solid line: VCD spectra; dashed line: noise level).



**Fig. S19** Five groups solid-state VCD spectra of **Form-O** of **1b** under the same measuring condition (solid line: VCD spectra; dashed line: noise level).



**Fig. S20** Computed IR and VCD spectra (solid line) of **Form-Y** (black) and **Form-O** (blue) of complex **1a** compared to observed solid-state VCD spectra (dash line).

**Table S1** Structural parameters both solid-state forms of complexes **1a** and **1b** determined by X-ray single crystal diffraction.

| Bond Length | <b>1a-Form-Y</b> | <b>1a-Form-O</b> | <b>1b-Form-Y</b> | <b>1b-Form-O</b> |
|-------------|------------------|------------------|------------------|------------------|
| Pt1–C1      | 1.986(5)         | 1.991(4)         | 2.007(6)         | 1.993(10)        |
| Pt1–C2      | 1.957(5)         | 1.975(4)         | 1.985(12)        | 1.965(10)        |
| Pt1–N1      | 1.988(4)         | 1.988(3)         | 1.968(10)        | 1.968(8)         |
| Pt1–N2      | 2.111(4)         | 2.103(3)         | 2.088(10)        | 2.086(9)         |
| Bond Angles | <b>1a-Form-Y</b> | <b>1a-Form-O</b> | <b>1b-Form-Y</b> | <b>1b-Form-O</b> |
| C1–Pt1–C2   | 99.6(2)          | 98.95(17)        | 100.2(4)         | 100.1(5)         |
| C1–Pt1–N1   | 82.44(18)        | 82.31(15)        | 81.3(3)          | 81.1(4)          |
| C1–Pt1–N2   | 160.75(16)       | 160.88(15)       | 158.8(4)         | 159.5(4)         |
| C2–Pt1–N1   | 176.7(2)         | 178.23(15)       | 177.9(4)         | 178.3(4)         |
| C2–Pt1–N2   | 99.68(19)        | 100.16(13)       | 101.0(5)         | 100.4(4)         |
| N1–Pt1–N2   | 78.35(16)        | 78.57(11)        | 77.4(4)          | 78.5(3)          |